Old Drugs for a Newly Emerging Viral Disease, COVID-19: Bioinformatic Prospective

Dr. Sudhir Kumar Mishra,

Principal, S.S. College, Jehanabad,

Email: innovationskmishra@gmail.com

Abstract

The COVID-19 outbreak caused by the SARS-CoV-2 virus in late 2019 and early 2020 comprises a serious pandemic threat worldwide. Given the severity of the disease and the fact that there is no approved cure for this infectious disease, it seems reasonable to search for better candidates' drugs among approved antiviral or even antibacterial drugs for their anti-COVID-19 capability in contrast to the currently approved drugs. The enzyme main protease of SARS-CoV-2 that plays an important role in the virus life cycle seems to be a good target for inhibition by drugs. Accordingly, in the present work by using the molecular docking method, I used the newly released coordinate structure of the protease as a target and 40 approved drugs from anti-viral, anti-parasite anti-malaria groups as ligands for docking experiments. Blind and active site-directed docking experiments were carried out on the optimized and equilibrated structure of protease at pH 7, 37 degrees centigrade of temperature, and 1 atmosphere of pressure. My results indicate that based on binding energy, percentage of binding site occupation, membrane transportability, and the maximum allowed dosage, erythromycin, clarithromycin, amprenavir, darunavir, cefixime, and tetracycline are among the enrolled drugs merit best parameters for clinical evaluation and their therapeutic potential in COVID-19 outbreak.

Keywords: Coronavirus, COVID-19 Outbreak, Docking, Antibiotics, Anti-HIV Drugs, Macrolides.

INTRODUCTION

Severe acute respiratory syndrome corona virus (SARSCOV-2) is known as the infection source for the outbreak of COVID-19 in 2019-2020 [1-4]. It is a positive-sense singlestranded RNA virus that caused a total of 75, 465 reported cases up to February 2020 in China [5-6]. Increased risk and fast spread of the disease comprise serious life-threatening issues worldwide. Fever, cough, and shortness of breath are the main symptoms of the disease that may eventually lead to pneumonia with a mortality rate of 1-3% [7-11]. Currently, there are no approved drugs for coronavirus infections. However, antiviral drugs such as inhibitors against protease, integrase, and or polymerase enzymes designed and are in advance studies for viral diseases[12-13]. Among these inhibitors, antiprotease inhibitors seem to act effectively in blocking virus replication and provide a promising treatment for SARS and MERS diseases. Given the protease's vital role in the virus life cycle and its maturation via functional protein production from their precursor, it seems to be a good target for drug design in viral infections as in COVID-19 infection as well. Based on available data in the PUBMED database (https://www.ncbi.nlm.nih.gov/pubmed/) SARS-CoV-2 protease, EC 3.4.2 is a protein with 305 residues compared to SARS-CoV protease with 306 amino acid residues. Sequence alignment using the EMBOSS Stretcher server (www.ebi.ac.uk) revealed that SARS-CoV-2 protease compared to SARS-CoV protease contains about 12 mutations along its sequence stretch as depicted in Scheme 1. These changes in SARS-CoV-2 protease sequence may be behind the different global architecture of protein and especially its binding site, in such a way that the localization of binding sites in SARS-CoV-2 shifted to neighbors' residues contrast to that's of SARS-CoV protease. Binding site survey for these two proteases using Computed Atlas of Surface Topography of proteins (http://sts.bioe.uic.edu/castp/) server confirmed these changes in enzyme binding sites. Table 1 represents the binding site residues for SARS-CoV and SARS-CoV-2 protease. It is clear that there are only three residue similarities between two enzymes at positions 140-142, therefore, different amino acid constituents elsewhere and geometry expectedly need different inhibitors with different stoichiometry. Based on this fact, it is necessary to search for different inhibitors for SARS-CoV-2 infections. This is the main objective of this study.

```
EMBOSS_001      1 SGFRKMAFPSGKVEGCMVQVTCGTTTLNGLWLDDTVYCPRHVICTAEDML      50
                  ||||||||||||||||||||||||||||||||||||-|||||||||:||||
EMBOSS_001      1 SGFRKMAFPSGKVEGCMVQVTCGTTTLNGLWLDDVVYCPRHVICTSEDML      50

EMBOSS_001     51 NPNYEDLLIRKSNHSFLVQAGNVQLRVIGHSMQNCLLRLKVDTSNPKTPK     100
                  ||||||||||||||:|:|||||||||||||||||:|:||||||:|||||
EMBOSS_001     51 NPNYEDLLIRKSNHNFLVQAGNVQLRVIGHSMQNCVLKLKVDTANPKTPK     100

EMBOSS_001    101 YKFVRIQPGQTFSVLACYNGSPSGVYQCAMRPNHTIKGSFLNGSCGSVGF     150
                  |||||||||||||||||||||||||||||||-||||||||||||||||||
EMBOSS_001    101 YKFVRIQPGQTFSVLACYNGSPSGVYQCAMRPNFTIKGSFLNGSCGSVGF     149

EMBOSS_001    151 NIDYDCVSFCYMHHMELPTGVHAGTDLEGKFYGPFVDRQTAQAAGTDTTI     200
                  ||||||||||||||||||||||||||||-|||||||||||||||||||||
EMBOSS_001    150 NIDYDCVSFCYMHHMELPTGVHAGTDLEGNFYGPFVDRQTAQAAGTDTTI     199

EMBOSS_001    201 TLNVLAWLYAAVINGDRWFLNRFTTTLNDFNLVAMKYNYEPLTQDHVDIL     250
                  |:||||||||||||||||||||||||||||||||||||||||||||||||
EMBOSS_001    200 TVNVLAWLYAAVINGDRWFLNRFTTTLNDFNLVAMKYNYEPLTQDHVDIL     249

EMBOSS_001    251 GPLSAQTGIAVLDMCAALKELLQNGMNGRTILGSTILEDEFTPFDVVRQC     300
                  ||||||||||||||:|||||||||||||||||||.:||||||||||||||
EMBOSS_001    250 GPLSAQTGIAVLDMCASLKELLQNGMNGRTILGSALLEDEFTPFDVVRQC     299

EMBOSS_001    301 SGVTFQ      306
                  ||||||
EMBOSS_001    300 SGVTFQ      305
```

Scheme 1. Sequence alignment preformed on EMBOSS Stretcher (www.ebi.ac.uk) server. SARS-CoV-2 sequence is highlighted in yellow color.

METHODS AND MATERIALS

Coordinate Structures Retrieval and Preparations

Coordinate structures of SARS-CoV-2 protease with PDB ID 6LU7 in accordance with SARS-CoV protease with PDB ID 1UK3 were retrieved from protein data bank (https://www.rcsb.org/). The structures were obtained by the X-ray diffraction and refined at the resolutions of 2.16 Å and 2.4 Å, respectively. The structures were placed in separate rectangular boxes with dimensions of 8.15 × 9.06 × 9.58 nm and 9.44 × 9.26 × 10.63 nm dimensions, respectively. The two boxes were then filled with SPCE solvents with a water shell of 1.0 nm thickness. Steepest descent algorithm was used to minimize the system energy to lower than 200 kJ mol^{-1} . Energy minimization was performed at neutral pH (Asp, Glu, Arg and Lys ionized), 37 °C, and one atmospheric pressure [14-15]. Sequence Alignment was carried out for the two sequences of SARSCoV-2 and SARS-CoV protease on EMBOSS Stretcher (www.ebi.ac.uk) for comparison purposes [16-17].

Table 1. Active Site Residues Extracted from Computed Atlas of Surface Topography of Proteins
(http://sts.bioe.uic.edu/castp/)

SARS-CoV	SARS-CoV (Continued)	SARS-CoV-2 Crystal structure	SARS-CoV-2 Optimised structure
Residue(No)	Residue(No)	Residue(No)	Residue(No)
PHE(3)	ASN(142)	THR(24)	
ARG(4)	ILE(152)	THR(25)	THR(25)
LYS(5)	ASP(153)	THR(26)	
MET(6)	TYR(154)	LEU(27)	LEU(27)
ALA(7)	ASP(155)	PRO(39)	
PHE(8)	GLU(290)	HIS(41)	HIS(41)
PRO(9)	PHE(291)	CYS(44)	CYS(44)
GLY(11)	PHE(294)	THR(45)	
LYS(12)	ASP(295)	SER(46)	
GLU(14)	VAL(297)	MET(49)	MET(49)
GLY(15)	ARG(298)	PRO(52)	PRO(52)
CYS(16)	GLN(299)	TYR(54)	TYR(54)
MET(17)	CYS(300)	PHE(140)	PHE(140)
VAL(18)	SER(301)	LEU(141)	LEU(141)
TRP(31)	GLY(302)	ASN(142)	ASN(142)
ALA(70)	VAL(303)	GLY(143)	GLY(143)
GLY(71)		SER(144)	SER(144)
ASN(72)			GLY(146)
ASN(95)		HIS(163)	HIS(163)
LYS(97)		HIS(164)	
PRO(99)		MET(165)	MET(165)
ALA(116)		GLU(166)	GLU(166)
TYR(118)		LEU(167)	
GLY(120)		PRO(168)	PRO(168)
SER(121)		HIS(172)	
PRO(122)		ASP(187)	ASP(187)
SER(123)		ARG(188)	ARG(188)
GLY(124)		GLN(189)	GLN(189)
SER(139)		THR(190)	THR(190)
PHE(140)			ALA(191)
LEU(141)		GLN(192)	GLN(192)

Coordinate structures of tested drugs including chloroquine, hydroxychloroquine, niclosamide, ivermectin, dicloxacillin, gemifloxacin, sulfamethoxazole, cefaclor, ciprofloxacin, moxifloxacin, doxycycline, ofloxacin, cefdinir, cefditoren, cefprozil, ceftriaxone, cefpodoxime, cefazolin, tetracycline, ceftizoxime, erythromycin, cefotaxime, clarithromycin, cefuroxime, cefixime,

azithromycin, emtricitabine, ritonavir, indinavir, tenofovir, nelfinavir, remdesivir, darunavir, amprenavir, lopinavir, baloxavir, efavirenz, saquinavir, tipranavir, and atazanavir were obtained from PubChem database (https://pubchem.ncbi.nlm.nih.gov/) in SDF format and converted to PDB format using Open Babel software (http://openbabel.org/). The structures then transferred to ArgusLab software (http://www.arguslab.com/) [18] and checked for their bonds and energy optimization.

Blind Docking Experiments

To survey the potential anchoring site on SARS-CoV-2 protease for drug binding and to verify them as binding sites based on their similarity and vicinity to enzyme active site, we performed blind docking experiments in Hex 8.0.0 (http://www.loria.fr/~ritchied/hex/)[19] installed in Linux operating system. In order to include the non-bonding interactions of hydrogen bonds and electrostatic forces as well as structural complimentary of compound to enzyme active site, the default setting for Shape only, Sahpe + Electrostatic and Shape + Electrostatic + DARS, with macro sampling were used in separate experiments on optimized structures of protease and drugs as ligands. The best pose and the binding energies of the 100 poses were recorded for statistical analysis.

Active Site-Directed Docking

This kind of docking was performed using ArguLab [18] in default setting using the Lamarckian Genetic Algorithm with Max Generations: 10000 and binding site size: $17.96 \times 19.78 \times 26.44$ angstroms. The binding energies for the best 20 poses were extracted in Kcal mol-1 for further statistical analysis.

LogP for Drugs

Partition coefficient or logP shows the hydrophobic or hydrophilic character of molecules. Positive values of logP denote hydrophobic and negative values correspond to hydrophilic behavior for chemicals, however, logP = 0 indicates the even distribution of the chemicals between lipophilic and hydrophilic phase in solution. The logP for drugs was calculated on the Virtual Computational Chemistry Laboratory server (http://www.vcclab.org/) [20].

Data Handling and Analysis

All of the obtained numerical data were used in Excel and SPSS software. P-value under 0.05 was considered as the significance level.

RESULTS AND DISCUSSION

Sequence alignments for SARS-CoV-2 and SARS-CoV proteases revealed that there are twelve mutations along with SARS-CoV-2 protease as depicted in Scheme 1 by single or double dots instead of vertical lines.

Binding site survey revealed that these mutations in SARS-CoC-2 lead to structural alterations that shift the binding site to the residues in the SARS-CoV-2 protease sequence. Given that active site residues placed at flexible or hot points of the protein chain, the root mean square fluctuation (RMSF) plots for SARS-CoV-2 and SARS protease were obtained from molecular dynamic simulation to check this hypothesis. As shown in Fig. 1, the active sites with higher RMSF values is placed predominantly in the 140-192 region of SARS-CoV-2 protease, while in SARSCoV the active site residues are localized in 290-303 region of the sequence, which confirms our claim in this context. Therefore, it is not surprising when SARS-CoV inhibitors show no significant effects on SARS-CoV-2 inhibition in COVID-19 infections.

In Table 2, the percentage of binding site occupations by drugs for SARS-CoV-2 protease obtained from blind docking experiments is summarized. The drugs with more than 80% occupation including remdesivir, tetracycline, ceftizoxime, erythromycin, cefotaxime, clarithromycin, cefuroxime, darunavir, amprenavir, cefixime, lopinavir and azithromycin were selected for further studies.

In the next step, we carried out the active site-directed docking for the selected ligands in ArgusLab software to study the binding potency of ligands to fit the active site cavity. The binding energies obtained from our blind and active site-directed dockings in accordance with the percentage of binding site occupations for the selected drugs are shown in Table 3a. As indicated, lopinavir with -434.68 kJ mol^{-1} binding energy and 94% binding probability is expected to be the most powerful candidate for SARS-CoV-2 protease inhibition. Table 3b represents the partition coefficients for drugs as logP and the maximum allowed dosage for each drug in the clinic for treatment. As indicated in Table 3b, lopinavir with logP   of -5.51 reveals that this drug is a hydrophilic compound which may not easily reach intracellular protease for inhibition when contrasted to those having positive logP's. This fact may interpret why lopinavir cannot significantly affect sever states of COVID-19 as indicated by recent clinical trials [21-22].
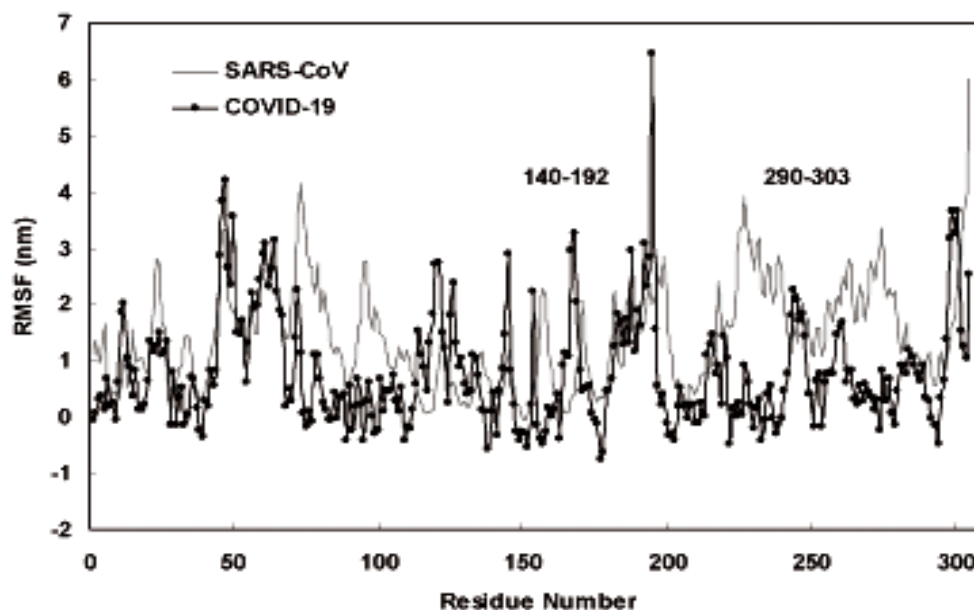
Fig. 1. Root Mean Square Fluctuation of proteases of SARS-CoV and SARS-CoV-2 obtained from 50 ns simulation at 37 degree centigrade, 1 atmosphere of pressure and pH 7.

Azithromycin with the binding energy of -421.50 kJ mol-1 and 95% binding to enzyme active site comprises the second probable candidate for enzyme inhibition (Table 2a). Based on logP of -3.16 for azithromycin, the drug is hydrophilic and seems again not to be suitable for COVID-19 treatment and protease inhibition The limited dosage of 0.5 g/day for azithromycin is the next obstacle in this context which restricts its effectiveness. However, there are clinical trials indicating that azithromycin can improve COVID-19 patients treated with hydroxychloroquine and decrease the viral load during treatment period. As indicated by some researchers, this effect of azithromycin is more probably caused by its antiinflammatory properties [23-25].

Clarithromycin and erythromycin are the next two volunteers with -403.25 and -393.54 kJ mol-1 binding energies, respectively. Both drugs are lipophilic with logPs' of 3.18 and 2.37, respectively. Therefore, these drugs are expected to reach protease freely by simple transport across cell membranes and inhibit the enzyme activity. Even though the binding energy of clarithromycin is significantly higher than that of erythromycin (p-value < .05), based on the higher allowed dosage of erythromycin of >1 g/day, in contrast to 0.5 g/day dosage for clarithromycin, we predict that the total effect of erythromycin in protease inhibition exceeds that of clarithromycin. Therefore, I suggest the priority of erythromycin for clinical trial consideration than clarithromycin. There are some clinical trials confirming the beneficial effect of clarithromycin in combination with chloroquine in COVID-19 patients; these findings are in good agreement with our calculations. However, there are no reports on erythromycin effects on COVID-19 patients [26-27].

Table 2. Percentage of Binding Site Occupation for 40 Drugs Enrolled in our Blind Docking Experiments in Hex 8.0.0

Drug	% of Occupation	Drug	% of Occupation
Dicloxacillin	0	Indinavir	54
Gemifloxacin	0	Cefditoren	57
Baloxavir	0	Tenofovir	57
Efavirenz	0	Cefprozil	60
Saquinavir	0	Nelfinavir	67
Tipranavir	4	Ceftriaxon	68
Cefaclor	8	Cefpodoxime	71
Ciprofloxacin	8	Cefazolin	77
Moxifloxacin	8	Remdesivir	83
chloroquine	15	Tetracycline	85
Niclosamide	16	Ceftizoxime	86
Hydroxychloroquine	23	Erythromycin	86
Atazanavir	23	Cefotaxime	87
Emtricitabine	24	Clarithromycin	91
Ritonavir	24	Cefuroxime	92
Sulfamethoxazole	28	Darunavir	92
Doxycycline	35	Amprenavir	93
Ofloxacin	44	Cefixime	94
Ivermectin	50	Lopinavir	94
Cefdinir	53	Azithromycin	95

Remdesivir, an antiviral drug that is currently approved for COVID-19 treatment in the USA, is placed in fifth priority in our series, considering its binding energy of -371.09 kJ mol^{-1} . I hypothesize that remdesivir with logP of -3.27 is a hydrophilic compound and maximum allowed dosage of effect on the advanced state of COVID-19, the problem which should be due to its transportation across the infected cells [28-29].

Table 3a. Active Site Occupation Percentages, and Binding Energies Obtained for Blind and Active Sites Directed Docking for the Studied Ligands as Well as Their Total Amount (in kJ mol-1) to SARS-CoV-2 Protease as Receptor

	% of Occupation	Blind docking	Active site	Total binding energy
Tetracycline	85	-233.14	-25.66	-258.80
Cefotaxime	87	-257.16	-26.12	-283.28
Amprenavir	93	-278.02	-27.58	-305.61
Darunavir	92	-288.89	-29.38	-318.28

Ceftizoxime	86	-294.34	-26.29	-320.63
Cefuroxime	92	-316.73	-28.96	-345.69
Cefixime	94	-332.51	-33.14	-365.66
Remdesivir	83	-346.14	-24.95	-371.09
Erythromycin	86	-368.17	-25.37	-393.54
Clarithromycin	91	-396.90	-6.39	-403.29
Azithromycin	95	-394.17	-27.33	-421.50
Lopinavir	94	-407.34	-27.33	-434.68

Table 3b. Maximum Applicable Dosages of Drugs Obtained, and Sorted logP for Selected Drugs

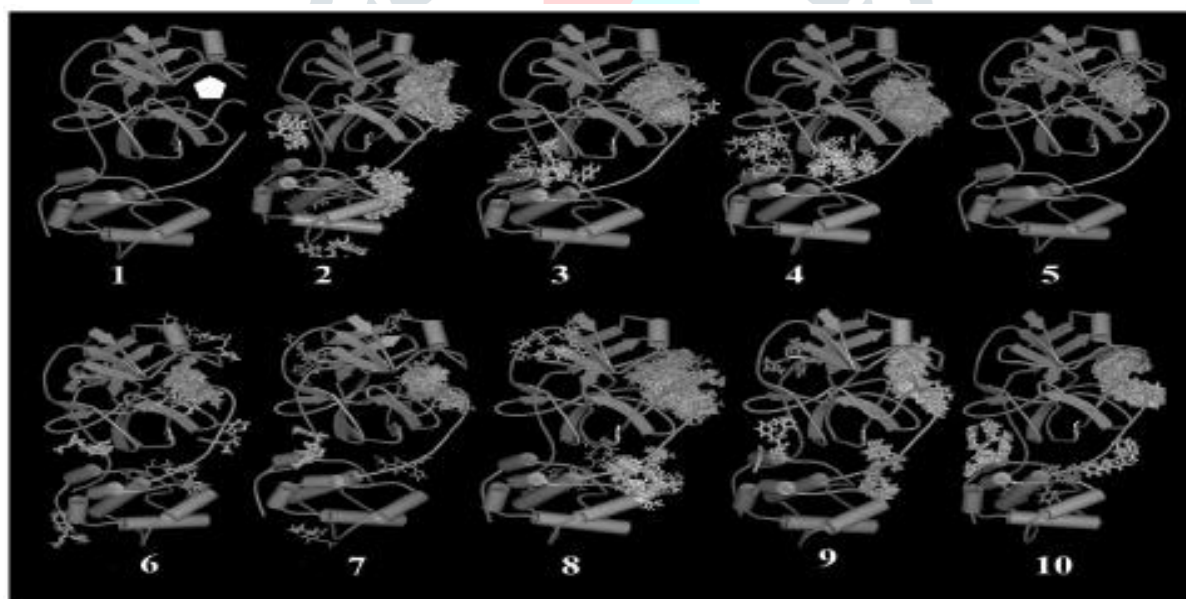|	Dosage (g/day)	logP
Lopinavir	<0.8	-5.51
Cefotaxime	>1	-3.49
Remdesivir	<0.2	-3.25
Ceftizoxime	>1	-3.22
Cefuroxime	0.5	-3.17
Azithromycin	0.5	-3.16
Tetracycline	>1	-0.56
Cefixime	0.8	0.25
Darunavir	0.8	1.89
Amprenavir	0.7	2.03
Erythromycin	>1	2.37
Clarithromycin	<1	3.18

Fig. 2. Graphical representation of (1) enzyme active sites and drugs binding patterns of 100 poses for (2) Amprenavir, (3) Azithromycin, (4) Cefixime, (5) Ceftizoxime, (6) Cefuroxime, (7) Clarithromycin, (8) Darunavir, (9) Lopinavir and (10) Remdesivir.

Cefixime with the total binding energy of -365.66 kJ mol^{-1} and 94% of active site occupation and logP of 0.25 and 0.8 g/day dosage can be suggested as a complementary drug for COVID-19 patients especially considering its antibiotic effects and its effectiveness in combating opportunistic bacterial infections in patients [30]. Table 3b also indicates that in the rest of selected drugs, the

amprenavir with -282.2 kJ mol^{-1} , logP of 2.03 and 0.7 g/day and darunavir with -318.25 kJ mol^{-1} , logP of 1.89 and 0.8 g/day dosages are the next drugs worthy to be tested as clinical trials in COVID-19 treatment. In the case of darunavir, some reports show that darunavir and amprenavir show no significant effect on COVID-19 infections[31-32]. Finally, cefuroxime, from second generation of cephalosporins and ceftizoxime and cefotaxime from the third generations of cephalosporins with binding energies of -345.69, -320.63 and -283.28 kJ mol^{-1} and active site occupation of 92, 86 and 87 percent, respectively, comprises the penultimate candidates in our series. These antibiotics resemble logP's in the ranges of -3.17 to -3.49 which make them be more hydrophilic drugs with less expected efficacy in protease inhibition and COVID-19 treatment, however, their clinical trial results remain to be studied in future. The last candidate in our series is tetracycline with the least binding energy of -258.80 kJ mol^{-1} and 85% of binding site cavity occupation. Marginal logP of -0.56 and high allowed dose of more than 1 g/day make tetracycline valuable for clinical trials in COVID-19 patients in the early phase of disease onset as recommended before [33].

Figure 2 graphically represents the binding patterns of the best 9 inhibitors of amprenavir, azithromycin, cefixime, ceftizoxime, cefuroxime, clarithromycin, darunavir, lopinavir, and remdesivir. As indicated, all the selected drugs mostly bind to the enzyme binding which reveals the selected drugs seem to be appropriate candidates for protease inhibition in COVID-19 patients.

CONCLUSIONS

My results indicate that there are structural differences between SARS-CoV-2 protease and SARS-CoV protease that alter the enzyme binding sites. These alterations cause the enzyme not to respond to anti-SARS-CoV protease inhibitors in treatment [47-48]. Accordingly and by re-examining HIV-1 protease and anti-bronchitis antibiotics,

I tried to find more effective inhibitors for COVID-19 treatment. I, therefore, suggest erythromycin, clarithromycin, amprenavir, darunavir, cefixime, and tetracycline for more clinical evaluations and their therapeutic potentials.

ACKNOWLEDGEMENTS

REFERENCES

1.   D. Paraskevis, E.G. Kostaki, G. Magiorkinis, G. Panayiotakopoulos, G. Sourvinos, S. Tsiodras, Infect Genet Evol. 79 (2020) 104212.

2.   A.E. Gorbalenya, S.C. Baker, R.S. Baric, R.J. de Groot, C. Drosten, A.A. Gulyaeva, B.L. Haagmans, C. Lauber, A.M. Leontovich, B.W. Neuman, D. Penzar, S. Perlman, L.L.M. Poon, D. Samborskiy I.A. Sidorov, I. Sola, J. Ziebuhr BioRxiv 2 (2020) 1.

3.   P. Zhou, X.L. Yang, X.G. Wang, B. Hu, L. Zhang, W. Zhang, H.R. Si, Y. Zhu, B. Li, C.L. Huang, H.D. Chen, J. Chen, Y. Luo, H. Guo, R.D. Jiang, M.Q. Liu, Y. Chen, X.R. Shen, X. Wang, X.S. Zheng, K. Zhao, Q.J. Chen, F. Deng, L.L. Liu, B. Yan, F.X. Zhan, Y.Y. Wang, G.F. Xiao, Z.L. Shi. Nature 579 (2020) 270.

4.   D.S. Hui, E.I Azhar, T.A. Madani, F. Ntoumi, R. Kock, O. Dar, G. Ippolito, T.D. Mchugh, Z.A. Memish, C. Drosten, A. Zumla, E. Petersen, Int. J. Infect. Dis. 91 (2020) 264.

5.   World Health Organization (WHO). Archived from the Original on 20 January 2020. Retrieved 27 January 2020 .

6.   H.J. Wang, S.H. Du, X. Yue, C.X. Chen, F. Y. Xue, Z. Zhi, 36 (2020) 16.

7.   K.C. Liu, P. Xu, W.F. Lv, X.H. Qiu, J.L. Yao, J.F. Gu, W. Wei, Eur. J. Radiol. 2020 May;126:108941. doi: 10.1016/j.ejrad.2020.108941.

8.   S.A. Lauer, K.H. Grantz, Q. Bi, F.K. Jones, Q. Zheng, H.R. Meredith, A.S. Azman, N.G. Reich, J. Lessler, Ann. Intern. Med. 5 (2020) 577.

9.   S. Kannan, P. Shaik Syed Ali, A. Sheeza, K. Hemalatha, Eur. Rev. Med. Pharmacol. Sci. 24 (2020) 2006.

10. T. Singhal, Indian J. Pediatr. 87 (2020) 281.

11. M. Xie, Q. Chen, Int. J. Infect. Dis. 94 (2020) 119.

12. K.O. Chang, Y. Kim, S. Lovell, A.D. Rathnayake, W.C. Groutas, Viruses 25 (2019) 197.

13. S.M. Thomasy, D.J. Maggs, Vet Ophthalmol. 19 (2016) 119.

14. C. Sheng, H. Ji, Z. Miao, X. Che, J. Yao, W. Wang, G. Dong, W. Guo, J. Lü, W. Zhang, J. Comput. Aided Mol. Des. 23 (2009) 375.

15. G. Macindoe, L. Mavridis, V. Venkatraman, M.D. Devignes, D.W. Ritchie, Nucleic Acids Res. 38 (2010) W445-9.

16. A.M. Wensing, V. Calvez, F. Ceccherini-Silberstein, C. Charpentier, H.F. Günthard, R. Paredes, R.W. Shafer, D.D. Richman, Top. Antivir. Med. 27 (2019) 111.

17. M.R. Dayer, M.S. Dayer, J. Biomed. Sci. 12 (2013) 67.

18. S. Joy, P.S. Nair, R. Hariharan, M.R. Pillai, In Silico Biol. 6 (2006) 601.

19. D.W. Ritchie, D. Kozakov, S. Vajda, Bioinformatics. 24 (2008) 1865.

20. I.V. Tetko, J. Gasteiger, R. Todeschini, A. Mauri, D. Livingstone, P. Ertl, V.A. Palyulin, E.V. Radchenko, N.S. Zefirov, A.S. Makarenko, V.Y. Tanchuk, V.V. Prokopenko, J. Comput. Aided Mol. Des. 19 (2005) 453.

21. H. Stower, Nat. Med. 26 (2020) 465.

22. B. Cao, Y. Wang, D. Wen, W. Liu, J. Wang, G. Fan, L. Ruan, B. Song, Y. Cai, M. Wei, X. Li, J. Xia, N. Chen, J. Xiang, T. Yu, T. Bai, X. Xie, L. Zhang, C. Li, Y. Yuan, H. Chen, H. Li, H. Huang, S. Tu, F. Gong, Y. Liu, Y. Wei, C. Dong, F. Zhou, X. Gu, J. Xu, Z. Liu, Y. Zhang, H. Li, L. Shang, K. Wang, K. Li, X. Zhou, X. Dong, Z. Qu, S. Lu, X. Hu, S. Ruan, S. Luo, J. Wu, L. Peng, F. Cheng, L. Pan, J. Zou, C. Jia, J. Wang, X. Liu, S. Wang, X. Wu, Q. Ge, J. He, H. Zhan, F. Qiu, L. Guo, C. Huang, T. Jaki, F.G. Hayden, P.W. Horby, D. Zhang, C. Wang, N Engl. J. Med. 382 (2020) 1787.

23. P. Gautret, J.C. Lagier, P. Parola, V.T. Hoang, L. Meddeb, M. Mailhe, B. Doudier, J. Courjon, V. Giordanengo, V.E. Vieira, H. Tissot Dupont, S. Honoré, P. Colson, E. Chabrière, B. La Scola, J.M. Rolain, P. Brouqui, D. Raoult, Int. J. Antimicrob. Agents. 56 (2020) 105949.

24. S.S. Jean, P.I. Lee, P.R. Hsueh, J. Microbiol. Immunol. Infect. 53 (2020) 436.

25. World Health Organization (2019). World Health Organization Model List of Essential Medicines: 21st List 2019. Geneva: World Health Organization. hdl:10665/325771. WHO/MVP/EMP/IAU/2019.06. License: CC BY-NC-SA 3.0 IGO.

26. J. Millán Oñate, W. Millan, L.A. Mendoza, C.G. Sánchez, H. Fernandez Suarez, D.K. Bonilla Aldana, A.J. Rodríguez Morales, Ann. Clin. Microbiol. Antimicrob, 19 (2020) 16.

27. M.S. Whitman, A.R. Tunkel, Infect. Control. Hosp. Epidemiol. 13 (1992) 357.

28. J.A. Al-Tawfiq, A.H. Al-Homoud, Z.A. Memish, Travel Med. Infect. Dis. 34 (2020) 101615.

29. Y. Wang, D. Zhang, G. Du, R. Du, J. Zhao, Y. Jin, S. Fu, L. Gao, Z. Cheng, Q. Lu, Y. Hu, G. Luo, K. Wang, Y. Lu, H. Li, S. Wang, S. Ruan, C. Yang, C. Mei, Y. Wang, D. Ding, F. Wu, X. Tang, X. Ye, Y. Ye, B. Liu, J.Yang, W. Yin, A. Wang, G. Fan, F. Zhou, Z. Liu, X. Gu, J. Xu, L. Shang, Y. Zhang, L. Cao, T. Guo, Y. Wan, H. Qin, Y. Jiang, T. Jaki, F.G. Hayden, P.W. Horby, B. Cao, C. Wang, Lancet. 395 (2020) 1569 .

30. R.N. Brogden, D.M. Campoli-Richards, Drugs 38 (1989) 524.

31. J. Chen, L. Xia, L. Liu, Q. Xu, Y. Ling, D. Huang, W. Huang, S. Song, S. Xu, Y. Shen, H. Lu, Open Forum Infect. Dis. 7 (2020) 1.

32. S. De Meyera, D. Bojkovab, J. Cinatlb, E. Van Dammea, C. Buycka, M. Van Loocka, B. Woodfallc, S. Ciesekb, Int. J. Infect. Dis. 97 (2020) 7.

33. M. Sodhi, M. Etminan, Pharmacotherapy 40 (2020) 487